





In silico assessment of the potential of basalt amendments to reduce N₂O emissions from bioenergy crops

Elena Blanc-Betes^{1,2,3}  | Ilsa B. Kantola^{1,2,4} | Nuria Gomez-Casanovas^{1,2,3}  |
 Melennie D. Hartman⁵ | William J. Parton⁵ | Amy L. Lewis⁴ | David J. Beerling⁴  |
 Evan H. DeLucia^{1,2,3,4,6} 

¹Institute for Sustainability, Energy, and Environment, University of Illinois at Urbana-Champaign, Urbana, IL, USA

²Center for Advanced Bioenergy and Bioproducts Innovation, University of Illinois at Urbana-Champaign, Urbana, IL, USA

³Carl R. Woese Institute for Genomic Biology, University of Illinois at Urbana-Champaign, Urbana, IL, USA

⁴Leverhulme Centre for Climate Change Mitigation, Department of Animal and Plant Sciences, University of Sheffield, Sheffield, UK

⁵Natural Resource Ecology Laboratory, Colorado State University, Fort Collins, CO, USA

⁶Department of Plant Biology, University of Illinois at Urbana-Champaign, Urbana, IL, USA

Correspondence

Evan H. DeLucia, Institute for Sustainability, Energy, and Environment, University of Illinois at Urbana-Champaign, Urbana, IL, USA.
 Email: delucia@illinois.edu

Funding information

Leverhulme Trust, Grant/Award Number: RC-2015-029; US Department of Energy, Grant/Award Number: DE-SC 18420

Abstract

The potential of large-scale deployment of basalt to reduce N₂O emissions from cultivated soils may contribute to climate stabilization beyond the CO₂-removal effect from enhanced weathering. We used 3 years of field observations from maize (*Zea mays*) and miscanthus (*Miscanthus × giganteus*) to improve the nitrogen (N) module of the DayCent model and evaluate the potential of basalt amendments to reduce N losses and increase yields from two bioenergy crops. We found 20%–60% improvement in our N₂O flux estimates over previous model descriptions. Model results predict that the application of basalt would reduce N₂O emissions by 16% in maize and 9% in miscanthus. Lower N₂O emissions responded to increases in the N₂:N₂O ratio of denitrification with basalt-induced increases in soil pH, with minor contributions from the impact of P additions (a minor component of some basalts) on N immobilization. The larger reduction of N₂O emissions in maize than in miscanthus was likely explained by a synergistic effect between soil pH and N content, leading to a higher sensitivity of the N₂:N₂O ratio to changes in pH in heavily fertilized maize. Basalt amendments led to modest increases in modeled yields and the nitrogen use efficiency (i.e., fertilizer-N recover in crop production) of maize but did not affect the productivity of miscanthus. However, enhanced soil P availability maintained the long-term productivity of crops with high nutrient requirements. The alleviation of plant P limitation led to enhanced plant N uptake, thereby contributing to lower microbial N availability and N₂O emissions from crops with high nutrient requirements. Our results from the improved model suggest that the large-scale deployment of basalt, by reducing N₂O fluxes of cropping systems, could contribute to the sustainable intensification of agriculture and enhance the climate mitigation potential of bioenergy with carbon capture and storage strategies.

KEYWORDS

agriculture, biogeochemical model, greenhouse gases, nitrogen cycle, soil phosphorus

1 | INTRODUCTION

Large-scale deployment of bioenergy with carbon capture and storage (BECCS) strategies is widely proposed to be a crucial element of climate risk management (Fuss et al., 2014; Kato & Yamagata, 2014; Obersteiner et al., 2018; Smith et al., 2016). Given the amplified global warming potential of N_2O (298 CO_2eq ; Foster et al., 2007), fertilizer-derived N_2O emissions from bioenergy crops could reduce climate savings by fossil fuel displacement, raising concerns about the efficacy of biofuels to abate global warming (Crutzen et al., 2016; Reay et al., 2012; Smith et al., 2019). Reducing the N_2O emission factor (EF; i.e., N_2O EF; percentage of N_2O -N emission relative to N fertilization) of cultivated land is critical for reaching climate targets sustainably (Davidson & Kanter, 2014; Reay et al., 2012; Tilman et al., 2011). The potential of basalt, a fast-reacting silicate rock commonly used in CO_2 removal strategies by enhanced weathering (Beerling et al., 2018; Taylor et al., 2016), to reduce N_2O losses from croplands (Kantola et al., in review) opens an opportunity to limit the non- CO_2 climate forcing of agriculture and enhances the climate mitigation potential of BECCS. However, the biogeochemical drivers of the response of N_2O fluxes to basalt remain unresolved, hampering a full assessment of the role of large-scale deployment of basalt in climate stabilization schemes.

The rapid weathering of basalt and accessory minerals releases base cations (Ca^{2+} , Mg^{2+} , Na^+ and K^+), which increase total alkalinity and raises soil pH, enhancing the bioavailability of essential nutrients such as phosphorous (P; Anda et al., 2015; Gillman et al., 2001, 2002; Kelland et al., 2020; MacDonald et al., 2011). Basalt amendments may reduce N_2O emissions either singly or in combination, by: (a) a P-driven increase of the nitrogen use efficiency (i.e., NUE; yield produced per unit of N applied; Ågren et al., 2012; Yu et al., 2017); and (b) a pH-driven decrease of the $\text{N}_2\text{O}:\text{N}_2$ ratio of denitrification by stimulating the activity of N_2O reductase, the enzyme responsible for reducing N_2O to N_2 (Figure 1; Mukumbuta et al., 2018; Rochester, 2003; Samad et al., 2016). By stimulating plant N uptake, P-driven

interactions could reduce total N losses and hence fertilizer requirements and the N_2O EF of cropping systems, whereas pH-driven interactions would maintain N losses but reduce the N_2O EF of cropping systems in favor of the emission of inert N species (N_2 ; Figure 1).

The impact of basalt on the N_2O emissions of cropping systems is likely regulated by C and nutrient bioavailability. Mehnaz et al. (2018) showed that P addition increased the $\text{N}_2\text{O}/\text{CO}_2$ of soil emissions under carbon (C)-limiting conditions but decreased this ratio with the addition of labile C, and Baral et al. (2014) found that the sensitivity of N_2O emissions to P additions increased with soil N availability. This context dependency represents a challenge to unraveling the relative contribution of increased P or pH in controlling N_2O emissions in basalt-treated crops.

Process-based ecosystem models are valuable tools for generating new hypotheses and revealing potential mechanisms that can lead to effective climate mitigation (Davis et al., 2010). Recognizing the dearth of empirical data demonstrating the effect of basalt on N_2O emissions and other soil properties, we used the biogeochemical model DayCent to evaluate the potential of basalt amendments to reduce N losses, increase yields, and reduce climate forcing from BECCS.

We performed an *in silico* assessment of the response of maize (*Zea mays*) and miscanthus (*Miscanthus × giganteus*) yields and N_2O fluxes to two different types of basalt, a higher P/lower alkali basalt and a lower P/higher alkali basalt. These two bioenergy crops have differing belowground C allocation patterns (low and high respectively), and nutrient cycling efficiencies and requirements (high and low respectively; Anderson-Teixeira et al., 2009; Davis et al., 2012; Kantola et al., 2017). Given the codependency of the sensitivity of N_2O fluxes to soil pH or P availability with labile C and nutrient content, different responses may be expected from maize and miscanthus to different basalt-induced changes in soil pH and P availability.

DayCent is a process-based model widely used to simulate biogeochemical processes in natural and managed systems (Campbell et al., 2014; Cheng et al., 2014; Davis

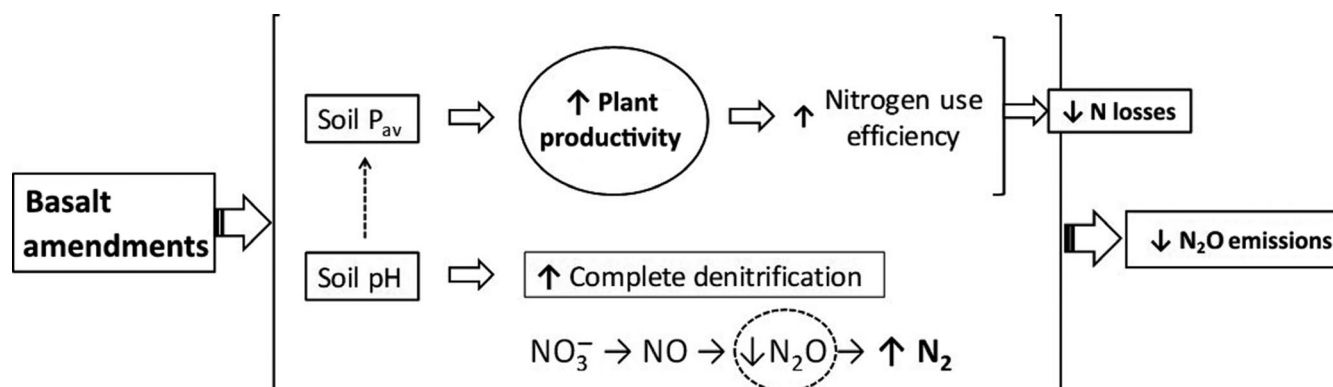


FIGURE 1 Conceptual model depicting key drivers of ecosystem responses to basalt amendments

et al., 2010; Del Grosso et al., 2005; Del Grosso, Halvorson, et al., 2008; Del Grosso, Parton, et al., 2008; Del Grosso, Wirth, et al., 2008; Del Grosso et al., 2009, 2011; Hudiburg et al., 2015, 2016; Parton et al., 1998). However, the model does not integrate regulating functions of soil pH on denitrification, the accuracy of simulated N_2O emissions relying on single point calibrations against fixed soil pH values. Given that denitrification is the predominant N_2O -producing process at the global scale (Davidson, 2009; Inatomi et al., 2019; Xu-Ri et al., 2012), failing to adequately capture the dynamic interaction of soil pH and the denitrification metabolism could result in strong biases in N_2O flux estimates over a wide range of soil pH, both spatially and over time. Prior to using the model to explore the effects of basalt addition on N_2O fluxes, it was modified to incorporate soil pH interactions with the total activity and end-product stoichiometry of denitrification by coupling pH with pre-existing denitrification functions. We tested model performance using data collected from control and basalt amended plots at the Energy Farm (UIUC) for maize and miscanthus. The new model was then used to (a) evaluate how much model performance improves with the incorporation of pH into the denitrification subroutine; (b) identify the dominant mechanisms driving the response of yields and N_2O fluxes to basalt; and (c) assess the potential of basalt amendments to improve the NUE and reduce the N_2O EF of maize and miscanthus. With an improved ability to capture the interactions of basalt with the nitrogen cycling of agricultural systems, the research presented here represents the first step toward the full appraisal of the climate mitigation potential of a promising, albeit understudied carbon dioxide removal strategy.

2 | MATERIALS AND METHODS

2.1 | Model description

The DayCent ecosystem model (Del Grosso, Parton, Mosier, Hartman, Brenner, et al., 2001; Del Grosso, Parton, Mosier, Hartman, Keough, et al., 2001; Kelly et al., 2000; Parton et al., 1998), the daily time step version of the CENTURY model, simulates the exchange of C, nutrients (N and P), and gases among the atmosphere, soil and plants as a function of light, temperature and water and nutrient availability. Primary model inputs are soil texture, current and historical land use, and daily weather. DayCent includes submodels for plant productivity, decomposition of dead plant material and soil organic matter (SOM), soil water and temperature dynamics, and N gas fluxes. The plant growth submodel simulates plant productivity as a function of nutrient availability, soil water and temperature, solar radiation, and plant-specific physiological parameters (e.g., potential growth, heat and

light tolerance, nutrient requirements; Del Grosso, Parton, et al., 2008). SOM is simulated as a sum of dead plant matter and three SOM pools with different C:N ratios defining their turnover times (i.e., active, slow, and passive; Kelly et al., 1997; Parton et al., 1993; Parton et al., 1994). The flow of C and nutrients among pools depends on the size and quality of these pools, temperature and water stress, and soil texture (Del Grosso et al., 2011; Parton et al., 1994). Decomposition of SOM and external nutrient additions supply the nutrient pool, which is in turn available for plant growth and microbial processes that result in trace gas fluxes. (Del Grosso, Parton, et al., 2008; Kelly et al., 1997; Parton et al., 1993).

The N gas submodel simulates soil N_2O , NO_x and N_2 gas emissions from nitrification and denitrification (Del Grosso et al., 2000; Parton et al., 1996, 2001). Daily nitrification simulates the oxidation of NH_4^+ to NO_3^- , with N_2O and NO_x released in the intermediate steps as a function of NH_4^+ concentration, temperature, pH, and water-filled pore space (WFPS). The nitrification rate is assumed to increase linearly with NH_4^+ concentration, to increase exponentially with soil temperature until the optimal temperature is reached and then decline, and to be limited by low soil pH, by water stress at low WFPS, and by O_2 availability at high WFPS (Parton et al., 1996, 2001). Daily denitrification simulates the stepwise reduction of NO_3^- to N_2 via NO and N_2O as a function of soil NO_3^- and labile C levels and is tightly regulated by O_2 availability (Del Grosso, Parton, Mosier, Hartman, Brenner, et al., 2001; Parton et al., 1996). The rate of denitrification increases exponentially with increasing soil NO_3^- concentration when NO_3^- concentration is low (<50 ppm) and linearly at higher NO_3^- concentration levels. Denitrification increases linearly with labile C availability. O_2 availability is simulated based on soil properties that describe gas diffusivity throughout the soil profile, soil WFPS, and O_2 demand dictated by respiration rates. Denitrification is assumed to be strongly limited at WFPS values below 50%–60%. The system becomes increasingly anaerobic under wetter soils increasing denitrification exponentially until WFPS reaches 70%–80% and the rate stabilizes as soil water content approaches saturation (Del Grosso, Parton, Mosier, Hartman, Keough, et al., 2001; Del Grosso, Wirth, et al., 2008; Parton et al., 1996).

N_2O and N_2 fluxes from denitrification are computed for each soil layer from total denitrification rates and built in $\text{N}_2:\text{N}_2\text{O}$ ratio functions. The $\text{N}_2:\text{N}_2\text{O}$ ratio is assumed to increase with decreases in NO_3^- -to-labile C ratio and O_2 availability, and with increases in the residence time of N_2O within a soil layer (represented as an increase in WFPS) favoring further reduction to N_2 (Del Grosso et al., 2000). Comparisons of model results and field observations show that DayCent reliably simulates biomass yields and SOM for various natural and managed systems, and N_2O and NO_3^- leaching data from

cropping systems show reasonable agreement with DayCent annual estimates (Abdalla et al., 2010; Davis et al., 2010; Del Grosso et al., 2005, 2006; Del Grosso, Halvorson, et al., 2008; Del Grosso, Parton, et al., 2008; Del Grosso, Wirth, et al., 2008; Del Grosso et al., 2009, 2010; Hudiburg et al., 2015, 2016).

2.2 | Model improvements

DayCent was modified to improve model performance by adjusting P solubility and interactions with soil pH and texture (Cabeza et al., 2017; Penn & Camberato, 2019), constraining P availability to plants (Christian et al., 2008; Faucon et al., 2010; Glaser & Lehr, 2019), and introducing soil pH in the regulation of the denitrification subroutine (Šimek & Cooper, 2002). Contrary to the reported negative correlation between soil pH and N₂O fluxes (Wang et al., 2018) and recently observed decreases in N₂O fluxes with basalt additions (Kantola et al., in review), the standard DayCent version predicted greater N₂O emissions with basalt-induced increases in soil pH led by enhanced nitrification rates, failing to capture the impacts of soil pH on denitrification, the dominant N₂O-producing mechanism in most soils (Šimek et al., 2002). The DayCent denitrification subroutine (Del Grosso et al., 2000; Parton et al., 1996) was therefore modified to incorporate responses to soil pH by: (a) reproducing the impacts of soil pH on gross denitrification rates (N₂ + N₂O); and (b) incorporating the impacts of soil pH on the stoichiometry of the end products of denitrification (N₂:N₂O ratio).

Total N loss during denitrification was computed assuming control by the limiting factor, soil NO₃⁻, or labile C availability (i.e., potential denitrification), constrained by O₂ availability and gas diffusivity defined by WFPS, and soil pH at each soil layer (Equation 1).

$$D_{\text{tot}} = \begin{cases} \max[0.066, \min[F_d(\text{NO}_3^-), F_d(\text{CO}_2)]] \times F_d(\text{WFPS}) \times F_d(\text{pH}) & \text{lyr} = 0, 1 \\ \min[F_d(\text{NO}_3^-), F_d(\text{CO}_2)] \times F_d(\text{WFPS}) \times F_d(\text{pH}) & \text{lyr} \geq 2 \end{cases} \quad (1)$$

where D_{tot} is the rate of denitrification per unit area (N₂ + N₂O production), $F_d(\text{NO}_3^-)$ is the maximum N flux per unit area for a given NO₃⁻ level, $F_d(\text{CO}_2)$ is the maximum N flux per unit area for a given heterotrophic respiration rate (proxy for labile C availability), and $F_d(\text{WFPS})$ and $F_d(\text{pH})$ are dimensionless functions that integrate the effect of soil moisture and pH on N flux, respectively.

Functions for $F_d(\text{NO}_3^-)$, $F_d(\text{CO}_2)$ and $F_d(\text{WFPS})$ are adapted from Parton et al. (1996) and later modifications described in detail in Del Grosso et al. (2000) (Equations 2–4):

$$F_d(\text{NO}_3^-) = 1.556 + \frac{76.91}{\pi} \times \arctan(\pi \times 0.00222 \times ([\text{NO}_3^-] - 9.23)) \quad (2)$$

where $[\text{NO}_3^-]$ is soil nitrate concentration (ppm N) calculated from the soil nitrate content (g N/m²) and the soil mass of each layer (g soil/m²) derived from bulk density (g/cm³) and layer thickness (cm).

$$F_d(\text{CO}_2) = \max \left[0.0, \left(0.1 \times [\text{CO}_2 - \text{corr}]^{1.3} - \min[\text{NO}_3^-] \right) \right] \quad (3)$$

where $[\text{CO}_2 - \text{corr}]$ is CO₂ concentration (ppm CO₂) computed from microbial soil respiration (g C m⁻² day⁻¹) and soil mass (g soil/m²) corrected for the soil gas diffusivity of each soil layer (Potter et al., 1996), and $\min[\text{NO}_3^-]$ is the minimum required nitrate concentration in a soil layer for denitrification (0.1 ppm N).

$$F_d(\text{WFPS}) = 0.45 + \frac{\arctan(0.6\pi(10.0 \times \text{WFPS} - a))}{\pi} \quad (4)$$

where a is a layer-specific inflection coefficient calculated from soil gas diffusivity and O₂ demand inferred from corrected CO₂ concentration at each soil layer.

The pH effect function, $F_d(\text{pH})$, was adapted from Wagena et al. (2017) with adjusted thresholds based on sensitivity limits reported in the literature (Liu et al., 2010; Šimek & Cooper, 2002; Šimek et al., 2002; Equation 5):

$$F_d(\text{pH}) = \begin{cases} 0.001 & \text{for pH} \leq 4 \\ (\text{pH} - 4)/3 & \text{for } 4 < \text{pH} < 7 \\ 1.0 & \text{for pH} \geq 7 \end{cases} \quad (5)$$

After computing total N flux from denitrification, the ratio of N₂:N₂O was calculated as a function of e⁻ acceptor (NO₃⁻) to substrate (labile C; proxy for e⁻ donor availability)

ratio regulated by WFPS and pH for each soil layer, and assumed a minimum value of 0.1 (Equation 6):

$$R_{\text{N}_2/\text{N}_2\text{O}} = \max \left[0.1, F_r(\text{NO}_3^-/\text{CO}_2) \times F_r(\text{WFPS}) \times F_r(\text{pH}) \right] \quad (6)$$

where $R_{\text{N}_2/\text{N}_2\text{O}}$ is the N₂ to N₂O ratio of the end products of denitrification, and $F_r(\text{NO}_3^-/\text{CO}_2)$, $F_r(\text{WFPS})$, and $F_r(\text{pH})$ describe the effects of the relative abundance of soil NO₃⁻ and CO₂, WFPS and pH on the N₂:N₂O ratio, respectively.

Functions from Del Grosso et al. (2000) were adapted for $F_r(\text{NO}_3^-/\text{CO}_2)$ and $F_r(\text{WFPS})$ (Equations 7 and 8), and

$F_r(\text{pH})$ was modified from Liu et al. (2010) and Rochester (2003) (Equation 9).

$$F_r \text{ NO}_3^-/\text{CO}_2 = \max \left[k \times 0.16, k \times \exp \frac{-0.8 \times [\text{NO}_3^-]}{[\text{CO}_2 - \text{corr}]} \right] \quad (7)$$

where k is a model-fitted coefficient with a minimum value of 1.5 that controls maximum $\text{NO}_3^-/\text{CO}_2$ based on soil gas diffusivity (Del Grosso et al., 2000).

$$F_r(\text{WFPS}) = \max [0.1, 1.5 \times \text{WFPS} - 0.32] \quad (8)$$

$$F_r(\text{pH}) = 0.0016 \times \exp(1.006 \times \text{pH}) \quad (9)$$

Denitrification N_2 and N_2O flux rates were then calculated from the sum of daily total N (ppm N) and $\text{N}_2:\text{N}_2\text{O}$ ratio of each soil layer converted to $\text{g N m}^{-2} \text{ day}^{-1}$ accounting for layer-specific soil mass.

The ability of $F_r(\text{pH})$ to reproduce the response of the $\text{N}_2:\text{N}_2\text{O}$ ratio to pH was tested independently against direct observations from McMillan et al. (2016) and Mukumbuta et al. (2018; Figure S1). The accuracy of the new model was tested by regressing simulated data against randomly selected observations of plant productivity, yields, P availability, N_2O emissions, and N leachates for maize and miscanthus plots at the Energy Farm excluded from model calibration (Kantola et al., in review). Coefficients of determination (r^2), root mean square error (RMSE), bias, and deviation were used to evaluate the percentage of variation explained by the model and the accuracy of the prediction. Bias was defined as the tendency for model output to overestimate low values and underestimate high values. Bias was small when the slope approached 1 and the intercept approached 0. Deviation was calculated as the difference between simulated and measured values divided by the measured value.

2.3 | Model calibration

DayCent was calibrated for maize and miscanthus growing at the University of Illinois Energy Farm, located in central Illinois (40.06°N, 88.19°W). For model simulations, we used site-specific reconstructions of historical daily climate (CRU/NCEP 1901–1979; Viovy, 2018) and daily weather records (DayMet 1980–2008; www.daymet.org; Thornton et al., 2016) to drive historical simulations. Daily weather data from onsite weather stations were used to capture climatic variability at the Energy Farm over the past 11 years (2008–2018). Historical agricultural simulations followed a native tallgrass prairie with light grazing and a short fire return interval followed by ca. 150 years of agricultural history. Agricultural history included corn–soy rotations, alfalfa, and

wheat under historical management practices. Simulated soil carbon and nutrient stocks represent the preagricultural native prairie levels with a subsequent decline following agricultural intensification toward current grain-based cropping systems. Following agricultural history, the Energy Farm simulations were run from 2008 to 2018 reproducing the site management. Soil texture, bulk density, and pH were parameterized based on onsite measurements at the Energy Farm (Anderson-Teixeira et al., 2009).

DayCent was calibrated for maize and miscanthus following improvements developed from field observations of above- and belowground net primary productivity and C allocation, tissue C:N ratios, and biomass and grain yields at the Energy Farm (Dohleman et al., 2012; Hudiburg et al., 2015). A simulated stand age effect (i.e., establishment and aging) was developed using additional crop submodel definitions for miscanthus (Arundale et al., 2014). For maize–maize–soybean rotations, DayCent simulations reproduced spring N fertilizer additions to maize at the Energy Farm ($168\text{--}202 \text{ kg N ha}^{-1} \text{ year}^{-1}$), with no fertilizer additions during the soybean year. Previous research suggests that the N fertilization of miscanthus has a detrimental environmental impact without significant yield improvement during the initial stages of development (Davis et al., 2015). Therefore, miscanthus was not fertilized for the first 7 years and a low fertilization rate was applied to mature miscanthus crops from 2014 to 2018 to compensate soil N depletion with repeated harvest ($56 \text{ kg N ha}^{-1} \text{ year}^{-1}$; Arundale et al., 2014; Lee et al., 2017). Additional N inputs included atmospheric N deposition ($0.6 \text{ g N m}^{-2} \text{ year}^{-1}$), N in plant residue, and symbiotic-N fixation (Davis et al., 2010; Hudiburg et al., 2015) and retranslocation of plant N at senescence for miscanthus (Heaton et al., 2009).

Basalt amendments were simulated considering potential to increase extractable phosphorus (P) and to release alkaline-earth oxides (i.e., CaO and MgO), whose double-charged base cations (Ca^{2+} and Mg^{2+}) allow for enhanced alkalizing potential, thereby increasing soil P availability and pH (Gillman et al., 2002). DayCent was parameterized to reproduce system dynamics in response to two different types of basalt applied at the Energy Farm: a coarse-grained higher P/lower alkaline basalt applied in 2016 (Cascade basalt: $p80 = 714 \mu\text{m}$; 1.47% P_2O_5 , 7.87% alkaline-earth oxide), and a fine-grained lower P/higher alkaline basalt applied in 2017 and 2018 (Blueridge metabasalt: $p80 = 267 \mu\text{m}$; 0.2% P_2O_5 , 11.54% alkaline-earth oxide; Figure S3; Tables S1–S3; Appendix A1). Cascade basalt originates in the Cascade Mountain Range, Oregon (Central Oregon Basalt Products, LLC); with a chemical index alteration of 38%, it is considered relatively unaltered. The mineralogy indicated a predominance of plagioclase and alkali-feldspar, with relatively high apatite and low CaO and MgO (Kelland et al., 2020; Tables S1 and S3; Appendix A1). Blueridge metabasalt was

mined from the Catoctin Greenstone Belt in Virginia (USGS, 2003; Rock Dust Local, LLC). With a chemical index alteration of 47%, Bluebridge basalt comprises a metamorphic mineral assemblage of chlorite, epidote, actinolite, and albite (Table S2). Though trace P (0.2%) is observed, no apatite is identified through X-Ray Diffraction (Tables S2 and S3; Appendix A1). Basalt amended plots received 7 g P/m² in 2016 and 0.5 g P/m² in 2017 and 2018, and increased soil pH by 0.3–0.5 on average (Kantola et al., in review). In the model, P additions were simulated as early spring fertilization events and changes in pH were introduced with a pH scalar that reproduced monthly variations in pH observed at both control and basalt-treated plots in maize and miscanthus at the Energy Farm (Kantola et al., in review).

2.4 | Model simulations and nitrogen use metrics

Basalt-induced N₂O reduction in maize and miscanthus was quantified using model estimates of mean annual N₂O efflux from basalt amended and untreated (control) crops. To evaluate contributions of each driver to basalt-induced decreases in the N₂O efflux, simulations were adjusted to reproduce the impacts of changes in soil pH and P additions at the Energy Farm, individually and in combination. To further assess response dynamics of N₂O emissions from maize and miscanthus cropland to each individual parameter we conducted a sensitivity analysis of soil pH (i.e., 0.3, 0.5, 0.7, 1.0 units above baseline) and P availability (i.e., 0.25, 0.5, 0.7, 1.56 g/kg above baseline) using step-wise increases within a range consistent with basalt-induced changes observed at the Energy Farm. Scenarios were run using a factorial randomization of 15 year weather records looped over 80 years for a total of 30 weather iterations to integrate climatic variability.

We calculated the predicted impact of basalt on the N₂O EF of maize and miscanthus from estimates of fertilizer-induced N₂O emission relative to N fertilization following recommended procedures by the IPCC (De Klein et al. 2006; Equation 10).

$$\text{N}_2\text{O EF} = \frac{\text{N}_2\text{O N}_{\text{fert}} - \text{N}_2\text{O N}_{\text{unfert}}}{\text{N applied}} \quad (10)$$

The predicted effect of basalt amendments on nitrogen use in relation to crop yield was calculated from estimates of NUE (kg biomass/kg N; Equation 11) and apparent N recovery (ANR, %; Equation 12) for maize and miscanthus as the system's physiological efficiency and apparent recovery efficiency respectively (Fageria & Baligar, 2005).

$$\text{NUE} = \frac{\text{Yield}_{\text{fert}} - \text{Yield}_{\text{unfert}}}{\text{N applied}} \quad (11)$$

$$\text{ANR} = \frac{\text{Removed N}_{\text{fert}} - \text{Removed N}_{\text{unfert}}}{\text{N applied}} \times 100 \quad (12)$$

where Yield_{fert} and Yield_{unfert} are yield values with and without fertilizer additions, and Removed N_{fert} and Removed N_{unfert} are values of N removed in biomass during harvest with and without fertilizer N additions, respectively. Model output for unfertilized N₂O emissions, yields, and removed N were obtained from duplicated simulations without N additions.

Model outputs are reported as mean annual values. We calculated uncertainty using the error propagation equations described in the 2006 IPCC guidelines. Uncertainty was estimated for each crop and scenario considering variance over 80 year simulations and the error was propagated across 30 randomized weather iterations to integrate climate variability.

3 | RESULTS

3.1 | Model performance following implementation of the denitrification subroutine

Modification to the denitrification subroutine of the DayCent biogeochemical model led to improved predictions of daily N₂O emissions from maize and miscanthus both in control and in response to amendments with two types of basalt with different P and alkaline-earth oxide content (Figure 2). When compared with observations, predictions prior to model improvement overestimated daily N₂O fluxes from control maize and miscanthus by 29% and 45%, respectively. The new model reduced RMSE of predicted fluxes from 32.6 to 26.3, improving control N₂O flux estimates by 30% (Figure 2a,b). Standard DayCent showed greater uncertainty in the simulation of N₂O fluxes from basalt-treated soils than that from control, overestimating daily N₂O emissions by 71% and 116% from maize and miscanthus, respectively. Following calibration, the new subroutines reduced the RMSE of modeled N₂O fluxes from 27.9 to 17.8 and improved N₂O flux estimates from basalt amended soils by 60% (Figure S2). Model predictions of N₂O fluxes from both higher P/lower alkaline (Cascade) and lower P/higher alkaline (Bluebridge) basalt amended soils showed improved robustness relative to simulations prior to the incorporation of the impacts of soil pH on the denitrification subroutine, reducing RMSE from 24.2 to 20.7 (Figure 2c,d) and from 27.7 to 10.3 (Figure 2e,f), respectively. DayCent showed the largest improvement on the simulation of N₂O fluxes from soils with high alkalinity additions corresponding to scenarios with greater increases in soil pH (Bluebridge; Figure 1; Kantola et al., in review).

The new model effectively reproduced peak N₂O emissions following precipitation and fertilization events in control and basalt amended maize and miscanthus indicating the model

FIGURE 2 Observed versus DayCent simulated nitrous oxide (N_2O ; $\text{g N}_2\text{O-N ha}^{-1} \text{ day}^{-1}$) emissions for maize (black symbols) and miscanthus (white symbols) grown at the Energy Farm (UIUC) in control soils (dots, a and b) and soils treated with higher P/lower alkaline basalt (Cascade; triangles, c and d) and lower P/higher alkaline basalt (Blueridge; squares, e and f), before (standard DayCent) and after the integration of the impacts of soil pH on the denitrification subroutine

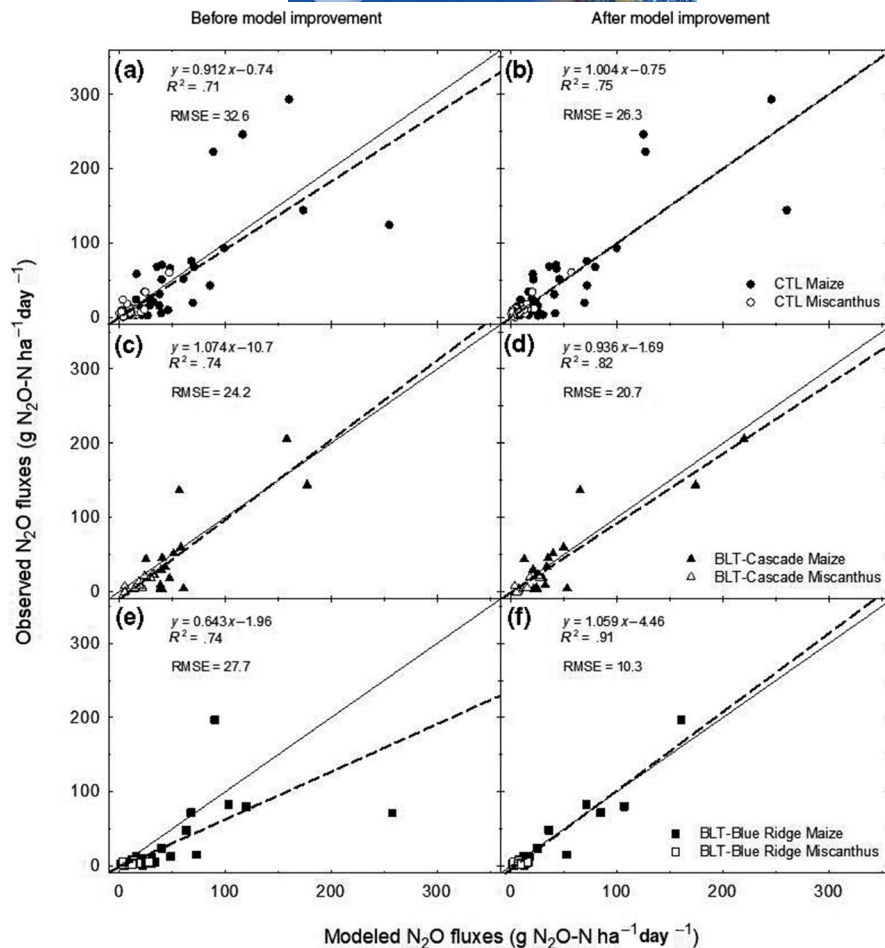
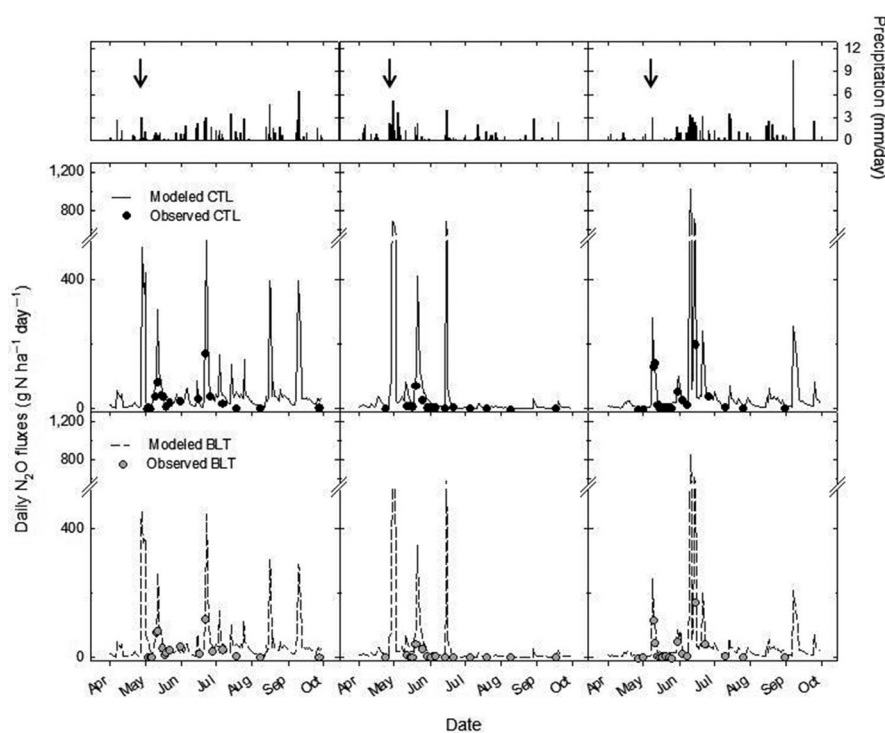


FIGURE 3 Daily precipitation (mm; top panel), and modeled (solid line) and observed (dots) daily N_2O fluxes ($\text{g N}_2\text{O-N ha}^{-1} \text{ day}^{-1}$; bottom panel) from maize at control (black; above) and basalt-treated (gray, below) plots at the Energy Farm over the growing seasons of 2016, 2017, and 2018. Arrows indicate timing of fertilization events



was successful in capturing the sensitivity of N_2O fluxes to soil hydrology and nutrient interactions (Figures 3 and 4). Model estimates show that denitrifier-derived N_2O accounts

for 68% to 72% of total net N_2O flux under control conditions. This is in agreement with previous research from adjacent fields at the Energy Farm showing that denitrification

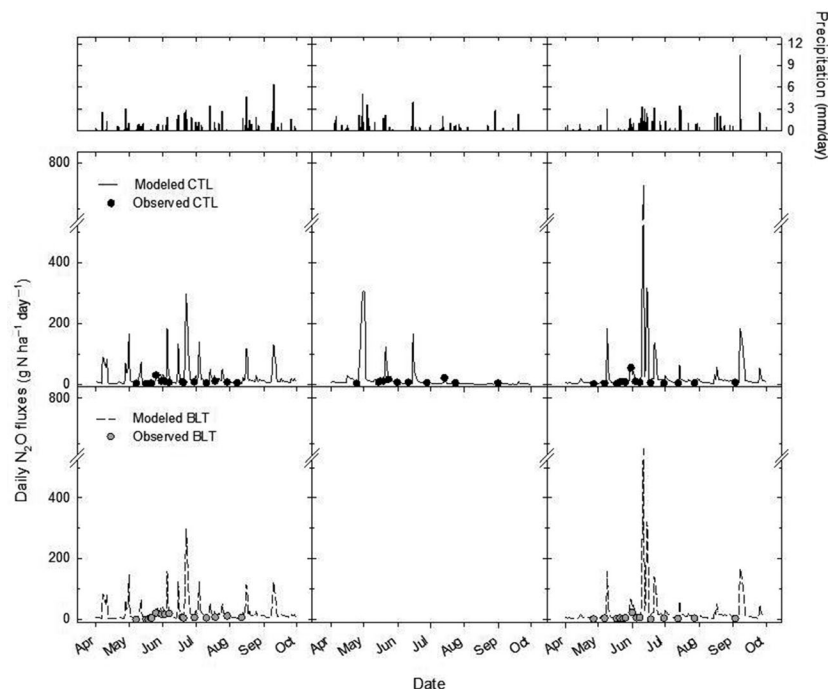


FIGURE 4 Daily precipitation (mm; top panel), and modeled (solid line) and observed (dots) daily N_2O fluxes ($g\ N_2O-N\ ha^{-1}\ day^{-1}$; bottom panel) from miscanthus at control (black; above) and basalt-treated (gray; below) plots at the Energy Farm over the growing seasons of 2016, 2017, and 2018. No basalt was applied to miscanthus in 2017. Arrows indicate timing of fertilization events

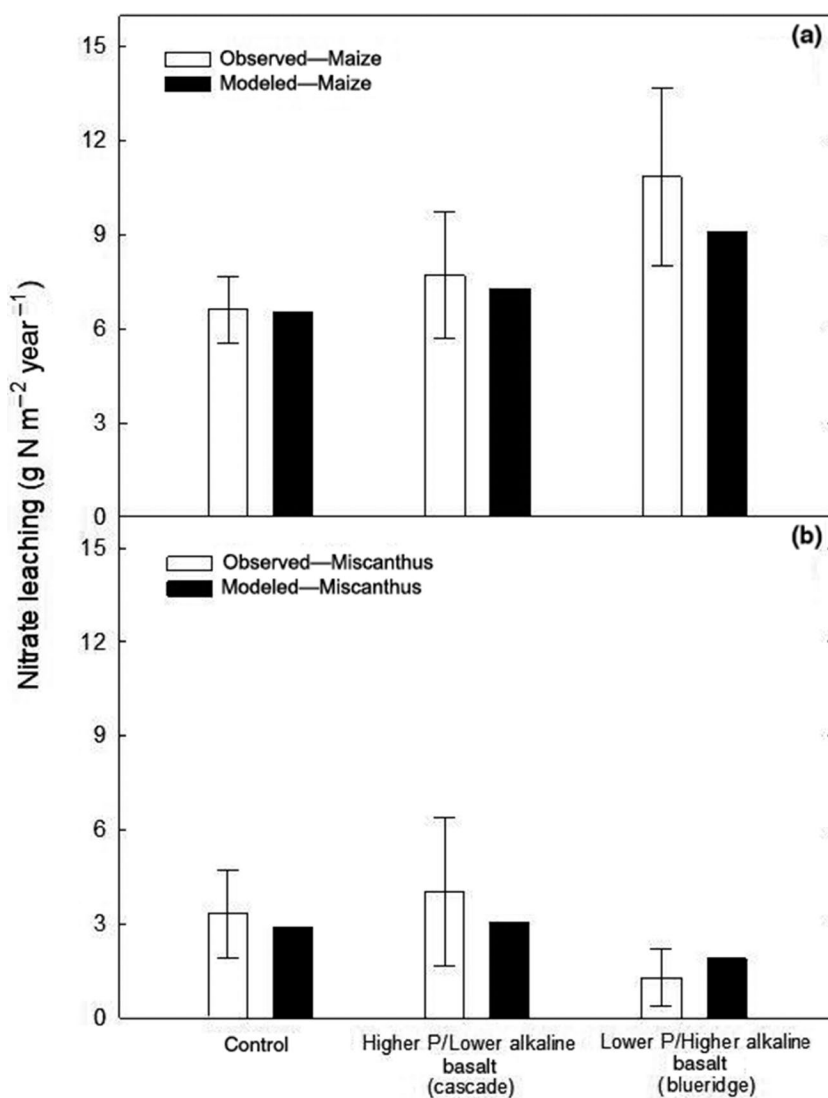


FIGURE 5 Observed (white) versus modeled (black) nitrate leaching ($g\ N\ m^{-2}\ year^{-1}$) for maize (a) and miscanthus (b) grown at the Energy Farm (UIUC) in control soils and soils treated with higher P/lower alkaline basalt (Cascade) and lower P/higher alkaline basalt. Error bars correspond to standard errors of the mean ($\pm SE$)

FIGURE 6 Observed (white) versus modeled (black) labile P ($\text{g P m}^{-2} \text{ year}^{-1}$) for maize grown at the Energy Farm (UIUC) in control soils and soils treated with higher P/lower alkaline basalt (Cascade) and lower P/higher alkaline basalt. Error bars correspond to standard errors of the mean ($\pm SE$)

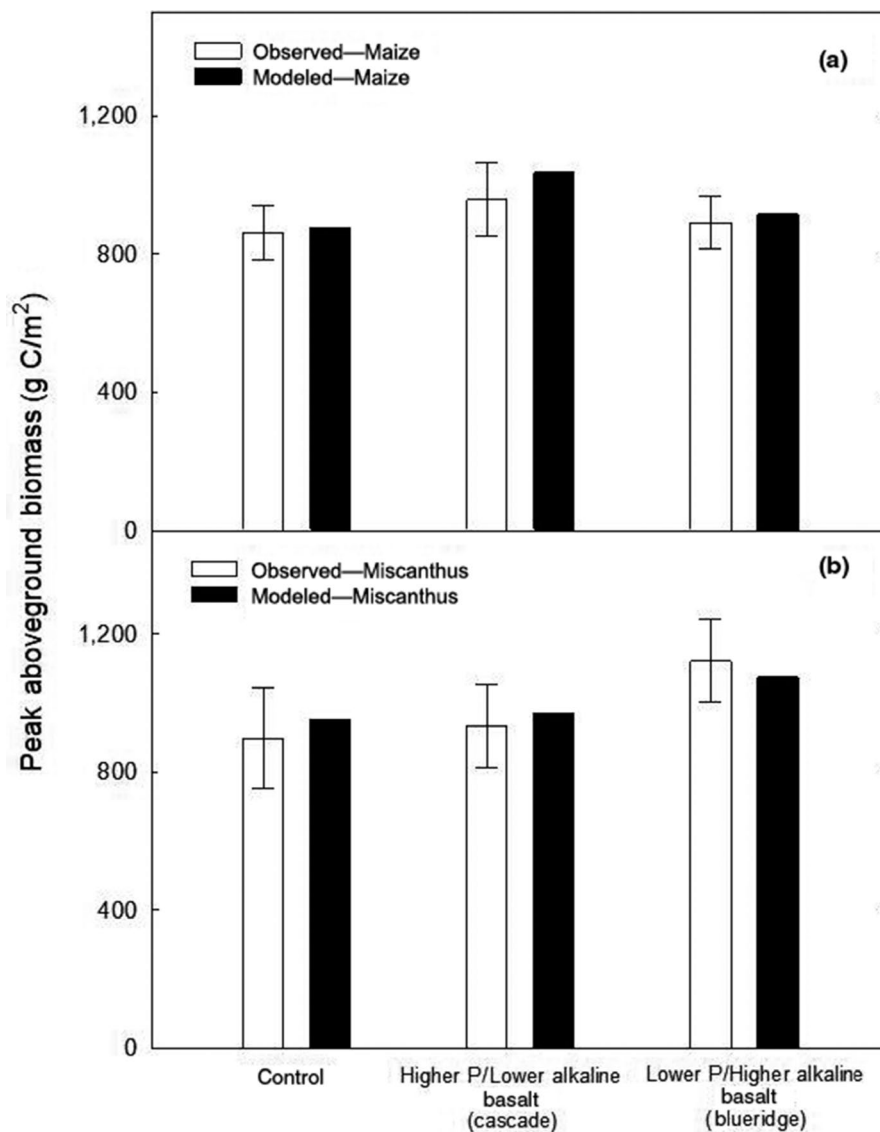
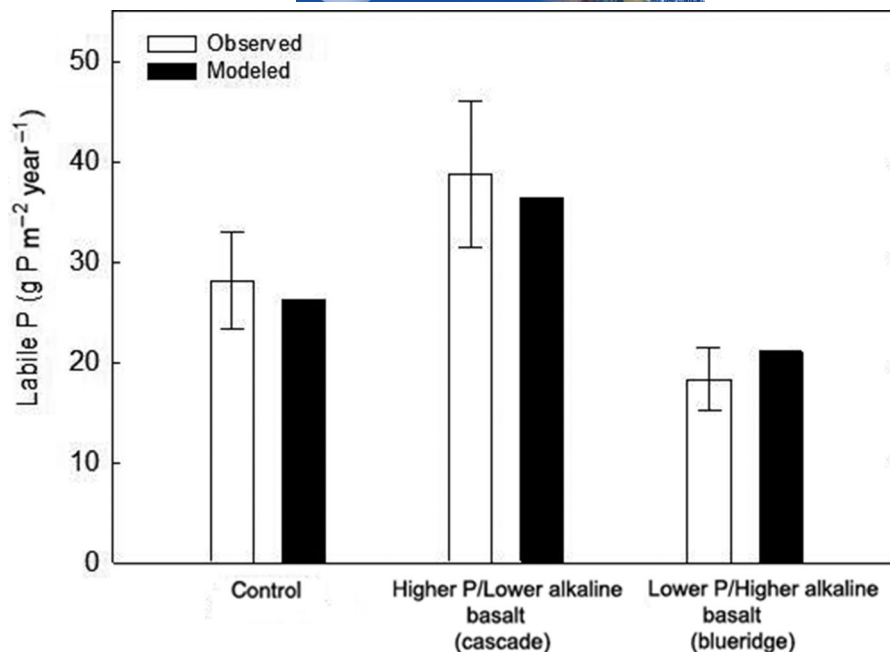


FIGURE 7 Observed (white) versus modeled (black) aboveground peak biomass (g C/m^2) for maize (a) and miscanthus (b) grown at the Energy Farm (UIUC) in control soils and soils treated higher P/lower alkaline basalt (Cascade) and lower P/higher alkaline basalt. Error bars correspond to standard errors of the mean ($\pm SE$)

contributes 72% of net N₂O emissions (Krichels et al., 2019), and indicates model robustness in reproducing the dynamics of the main contributing pathways to net N₂O emissions.

Model estimates of nitrate leaching and labile P compared favorably with measured values (Figures 5 and 6). Although there was both positive and negative model bias, differences between modeled and observed nitrate leaching were not statistically significant (two-sided $p > .05$), and the model successfully reproduced the response dynamics of nitrate leaching to both higher P/lower alkaline and lower P/higher alkaline additions in maize and miscanthus (Figure 5). Estimates of labile P also fell within 1 SE of observed values both at control plots and plots amended with basalt with different levels of P content and alkalinity (Figure 6).

Estimates of aboveground biomass compared well with measured values. Mean aboveground peak biomass showed a small bias (−4% to 8%) but varied little from observed means for control and basalt-treated maize and miscanthus, indicating the correct integration of the new subroutines with companion DayCent modules (Figure 7).

3.2 | Potential effects and drivers of basalt amendments

Integrating climate variability at the Energy Farm over 80 years, the new model predicted a mean annual N₂O efflux of 7.3 ± 0.3 for maize and 3.7 ± 1.6 kg N ha^{−1} year^{−1} for miscanthus control plots. Model estimates fall within the range reported from

the Energy Farm in the past decade for the same period ($3.4\text{--}7.7$ kg N/ha for maize and $0.6\text{--}1.4$ kg N/ha for miscanthus, from Apr to Oct; Smith et al., 2013). Simulated basalt additions reduced annual N₂O emissions to 6.1 ± 0.2 kg N ha^{−1} year^{−1} in maize and to 3.3 ± 0.6 kg N ha^{−1} year^{−1} in miscanthus, reducing the N₂O efflux of maize and miscanthus by 16.4% and by 8.5% on average, respectively (Figure 8).

Simulated individually, changes in soil pH and P availability showed different contribution to basalt-induced decreases in annual N₂O emissions. Contributions from each driver differed between maize and miscanthus. Basalt-induced increases in soil pH and P availability individually reduced the N₂O efflux of maize by 10.8% and by 4.2%, respectively (Figure 8a). However, decreases in annual N₂O emissions from basalt-treated miscanthus responded almost entirely to increases in soil pH, which reduced the N₂O efflux by close to 8.5% with negligible contributions from responses to P availability (<1%; Figure 8b). Modeled N₂O fluxes displayed a strong sensitivity to soil pH both in maize and in miscanthus, but the sensitivity to P availability differed among crops. N₂O fluxes were moderately sensitive to soil P content in maize and relatively insensitive in miscanthus (Figure 9). Annual N₂O emissions declined by 9.3%, 15.1%, and 30.8% in maize and by 3.9%, 8.2%, and 21.8% in miscanthus as the pH was raised 0.3, 0.5, and 1.0 above base conditions, respectively (Figure 9a,c). P additions reduced the N₂O emissions of maize by 2%–4% but the response rapidly saturated at loads above 5 g P m^{−2} year^{−1}, and N₂O emissions were irresponsive to changes in soil P content in miscanthus (Figure 9b,c).

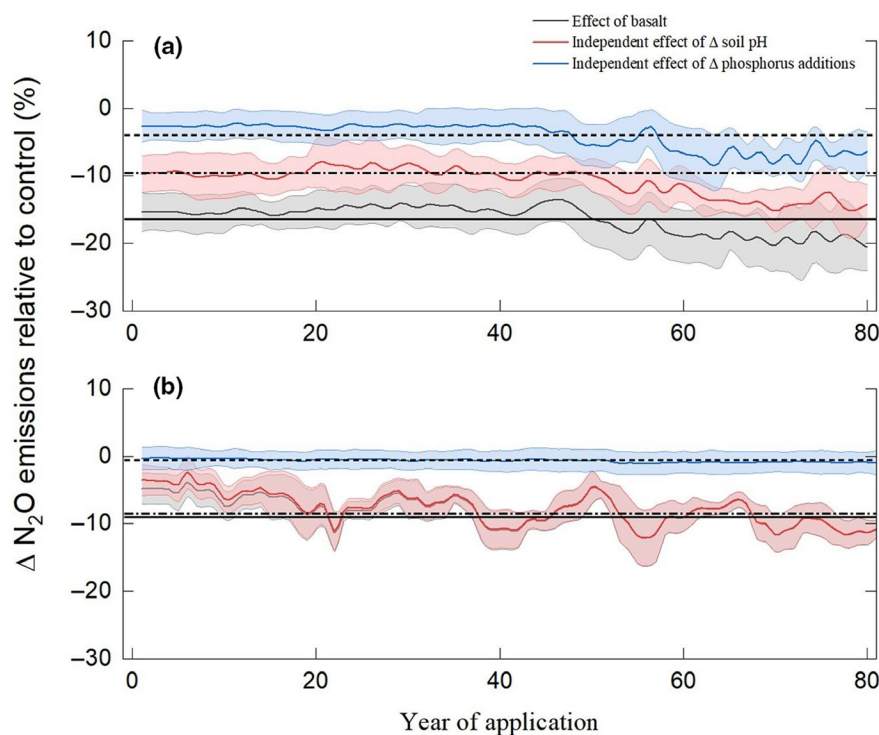


FIGURE 8 Model simulation of the long-term impacts (% change) of basalt amendments (solid line), and the independent effects of increases in soil pH (dashed line) and P content (dotted line) consistent with basalt amendments on annual N₂O emissions from maize (a) and miscanthus (b). Horizontal lines indicate mean effect relative to control (% change). Shaded areas integrate error propagation and indicate model uncertainty associated to climate variability

FIGURE 9 Model results of the response of annual N_2O emissions ($\text{kg N ha}^{-1} \text{ year}^{-1}$) from maize (a, b) and miscanthus (c, d) fields to stepwise increases in soil pH (black) and P additions (white)

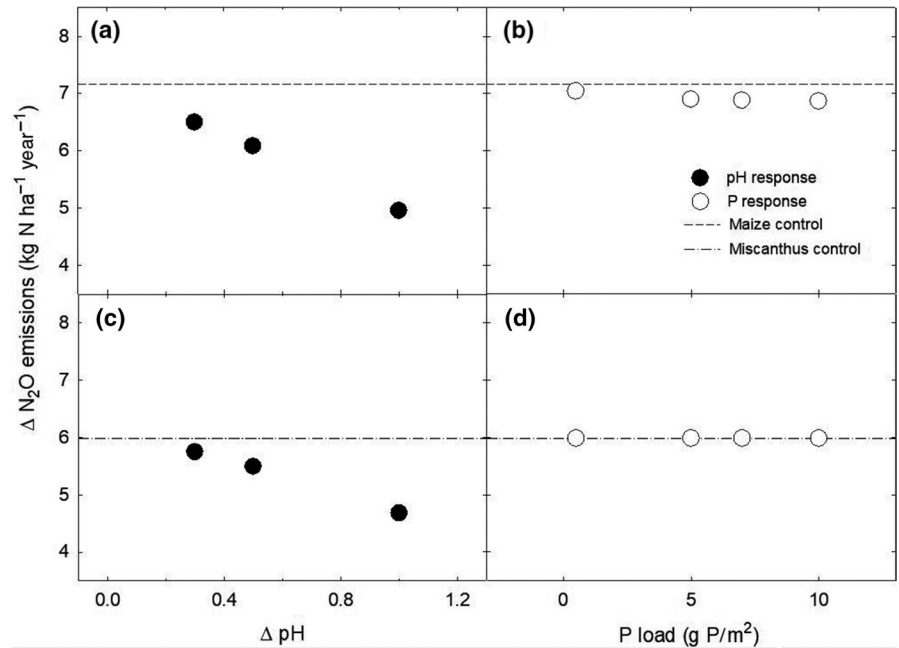


TABLE 1 Model estimates of mean annual productivity ($\text{Mg DW ha}^{-1} \text{ year}^{-1}$), yield ($\text{Mg DW ha}^{-1} \text{ harvest}^{-1}$) and harvested nitrogen ($\text{kg N ha}^{-1} \text{ harvest}^{-1}$) of maize (*Zea mays*) and miscanthus (*Miscanthus × giganteus*) over 80 year projections under control conditions without routine phosphorous additions (CTL), with basalt amendments (BLT), with increases in pH and available P consistent with basalt amendments (ΔpH and ΔP respectively), and under CTL and ΔpH with routine P fertilization consistent with current agricultural practices (CTL- P_{fert} and $\Delta\text{pH}-\text{P}_{\text{fert}}$ respectively). Reported values are mean estimates \pm standard errors of the mean. Standard errors of the mean ($\pm\text{SE}$) represent model uncertainty associated to climate variability. Different letters indicate significant differences among treatments ($p < .05$)

| | CTL | CTL- P_{fert} | BLT | ΔpH | $\Delta\text{pH}-\text{P}_{\text{fert}}$ | ΔP |
|-------------------------------|-------------------|-------------------------------|-------------------|-------------------|--|-------------------|
| <i>Zea mays</i> | | | | | | |
| Annual productivity | 14.6 ± 0.9^a | 20.2 ± 0.6^b | 21.6 ± 0.4^c | 14.5 ± 0.9^a | 20.1 ± 0.6^b | 21.5 ± 0.4^c |
| Grain yield | 8.7 ± 0.5^a | 12.0 ± 0.4^b | 12.9 ± 0.2^c | 8.6 ± 0.5^a | 12.0 ± 0.4^b | 12.8 ± 0.3^c |
| Harvested nitrogen | 110.1 ± 4.0^a | 136.0 ± 3.0^b | 142.4 ± 2.3^c | 109.3 ± 4.1^a | 135.5 ± 3.0^b | 142.0 ± 2.3^c |
| <i>Miscanthus × giganteus</i> | | | | | | |
| Annual productivity | 24.9 ± 0.7^a | | 25.0 ± 0.8^a | 25.0 ± 0.8^a | | 24.9 ± 0.7^a |
| Yield | 15.9 ± 0.5^a | | 16.0 ± 0.4^a | 16.0 ± 0.4^a | | 15.9 ± 0.5^a |
| Harvested nitrogen | 21.0 ± 0.6^a | | 21.1 ± 0.5^a | 21.1 ± 0.5^a | | 21.0 ± 0.6^a |

Basalt-induced increases in soil P content dominated the regulation of the long-term productivity and SOC of maize but did not affect those of miscanthus (Table 1). In the absence of alternative P sources, mean annual estimates of the aboveground productivity of maize and yields dropped by more than 30% under control and increased pH scenarios (Table 1). Routine P fertilization at loads reported for the Corn Belt region over the last decade (USDA, Economic Research Service, 2019), brought up the productivity of maize fully compensating long-term productivity losses, indicating that the decline in productivity was associated to P limitation (Table 1). Basalt amendments increased the mean annual productivity of maize by more than 10% above estimates of productivity under current management practices,

and similar increases were observed in P addition scenarios (Table 1). Similarly, modeled harvested N dropped by close to 25% in the absence of alternative P sources, whereas basalt amendments increased estimates of harvested N by close to 10% above that under current management practices (Table 1).

3.3 | Impacts of basalt amendments on N_2O EF, ANR, and NUE

Basalt-treated soils displayed lower EF both in maize and miscanthus, but the regulation of N fertilizer use in response to basalt differed between crops (Figure 10). Basalt amendments

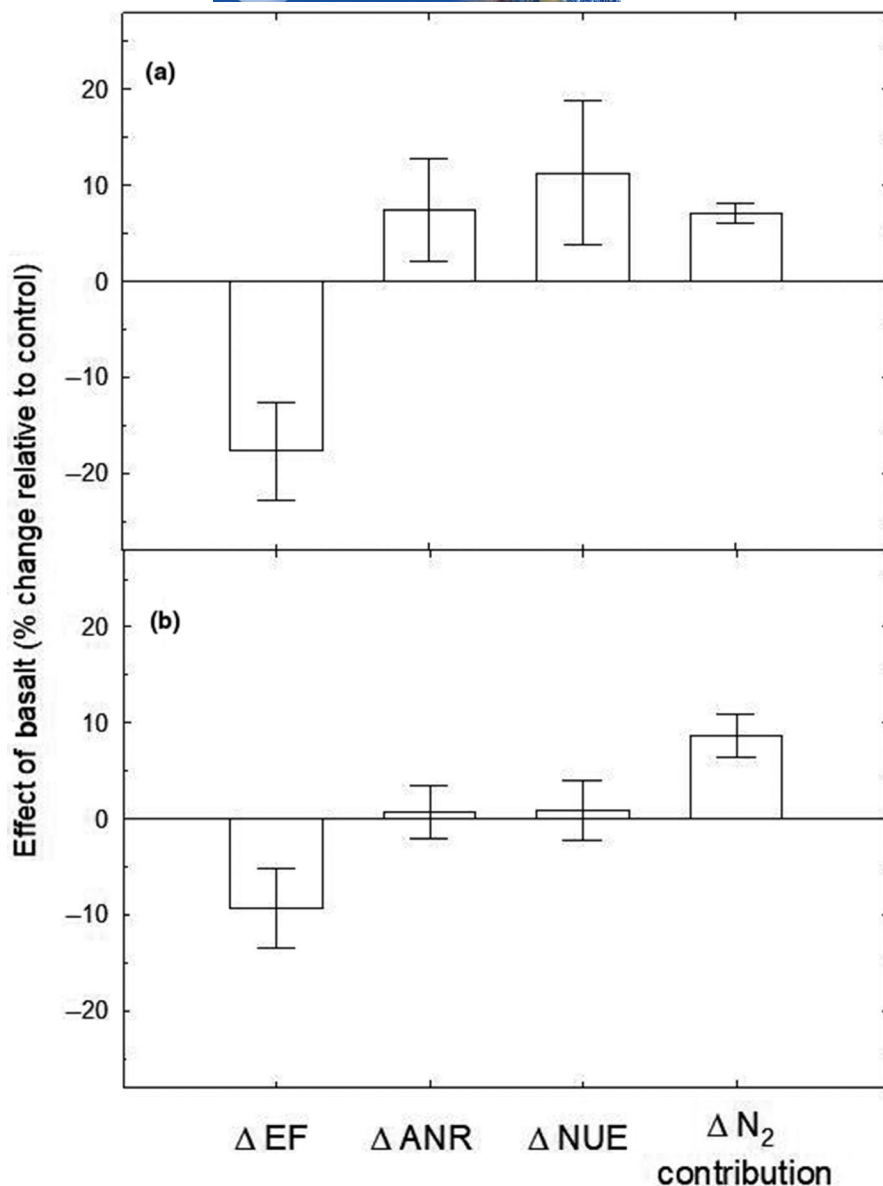


FIGURE 10 Model estimates of the impact of basalt amendments on the N_2O emission factor (ΔEF), apparent nitrogen recovery (ΔANR), nitrogen use efficiency (ΔNUE) and N_2 contributions to total ecosystem N emissions (ΔN_2 contribution) from maize (a) and miscanthus (b). Error bars correspond to standard errors of the mean ($\pm SE$) and integrate model uncertainty associated with climate variability

reduced the N_2O EF of cornfields by ~17% and increased the ANR and NUE of maize by about 7.5% and 11.3% respectively, the difference being largely explained by N losses through enhanced N_2 emissions (Figure 10a). Basalt reduced the EF of miscanthus by ~11% but had no significant impact on the ANR or the NUE, decreases in N_2O emissions being almost entirely compensated by increases in the emission of N_2 (Figure 10b).

4 | DISCUSSION

Adding process-based descriptions of the pH regulation of denitrification into the DayCent biogeochemical model and adjusting the effect of pH on the solubility of P within the model parameters, significantly improved the prediction of N_2O flux over previous versions of the model for soils at the Energy

Farm (Figure 2; Figure S1). Model results indicate that the application of basalt could reduce N_2O emissions and lower the N_2O EF from both maize and miscanthus, but the magnitude and the mechanisms mediating this response differed by crop. Predicted decreases in N_2O emissions responded to basalt-induced increases in soil pH with minor contributions from the impact of repeated P additions on N immobilization. Basalt amendments led to modest increases in modeled productivity, ANR, and NUE of maize with no significant effect in the productivity or nitrogen use of miscanthus. However, basalt-driven increases in soil P availability helped sustain the long-term productivity of crops with high nutrient requirements. Our findings suggest that basalt amendments have the potential to reduce the climate forcing of cultivated land beyond the CO_2 -removal effect from enhanced weathering.

Our results show significant improvement of model-data agreement of N_2O fluxes by incorporating a pH effect in the

denitrification subroutine, reducing model uncertainty by ~20% under control conditions, and by ~15% and by ~60% in the simulation of basalt amendments with low and high alkaline-earth oxide content, respectively (Figure 2). The new model accurately reproduced N_2O flux dynamics across a range of basalt-induced changes in soil pH and P content in two crops with different above- and belowground C allocation patterns, residue management, and nutrient cycling efficiencies and requirements grown at the Energy Farm (Figures 3 and 4). The evaluation of model performance in reproducing the response of codependent parameters (i.e., crop productivity, N leaching, labile P) indicates the correct integration of the new subroutines with companion DayCent modules (Figures 5–7), and increases our confidence that DayCent can adequately capture carbon and nitrogen response dynamics to changes in soil pH and P additions at levels consistent with basalt additions.

Our simulations indicate the potential of basalt amendments to significantly reduce the N_2O EF of both maize and miscanthus (Figure 10), but the mechanisms mediating these responses varied with crop type (Figures 8 and 9). Basalt-induced increases in soil pH dominated the response of N_2O emissions to basalt in both maize and miscanthus (Figure 8). This is consistent with recent studies identifying soil pH as a chief modifier of the N_2O EF of agriculture by regulating the activity of N_2O reductase and complete denitrification (Hénault et al., 2019; Samad et al., 2016; Wang et al., 2018). The N_2O response to N fertilizer inputs (ΔEF) grows significantly faster than linear for most crop types, including grain and perennial crops, and ΔEF is negatively correlated with soil pH (Shcherbak et al., 2014; Wang et al., 2018). Our results suggest the potential of basalt amendments to counter the amplification of N_2O emissions from intensive agricultural practices associated with progressive soil acidification. (Anda et al., 2015; Gillman et al., 2002). Our projections further indicate that the pH-driven mitigation effect is particularly important in intensively managed annual crops (Figure 8). Unlike miscanthus, a high nutrient efficiency perennial grass, maize is heavily fertilized ($130\text{--}220\text{ kg N ha}^{-1}\text{ year}^{-1}$ in the Corn Belt region of the United States), explaining the larger reduction of N_2O emissions in maize than in miscanthus (Figure 9) as the sensitivity of the $\text{N}_2\text{O}:\text{N}_2$ ratio to changes in pH increases with nitrate additions (Liu et al., 2010).

Basalt-driven additions of P to cultivated soils contributed to decreases in modeled N_2O emissions from maize but not from miscanthus (Figure 8). Decreases in N_2O emissions with P additions were accompanied by an enhanced NUE and a greater ANR of maize. This suggests that the alleviation of plant P limitation led enhanced plant N uptake reducing microbial N availability and N_2O emissions from crops with high nutrient requirements (Figure 10; Ågren et al., 2012; Schlegel et al., 1996), which is consistent with previous research showing up to 50% decreases in the N_2O

EF of nutrient-limited cropping systems with P fertilization (Baral et al., 2014). Similar “grain N-to-yield” ratios further suggest that the greater NUE and ANR of maize responded to enhanced productivity rather than to physiological adjustments of N allocation with increases in P availability (Table 1).

The observation that nutrient limitation regulated NUE and the suppression of N_2O emissions from maize systems is further supported by long-term projections of maize productivity. In the absence of an alternative source of P, the productivity of maize dropped by 35%–40% but these losses were recovered with routine P fertilization at loads consistent with application rates in the Corn Belt region of the United States over the past decade (Table 1; Cao et al., 2018; NASS, 2019; USDA, Economic Research Service, 2019). In a recent publication, Kelland et al. (2020) reported dissolution rates and mass transfer of elements from Cascade basalt weathering into the plant–soil system compatible with enhanced extractable P, sufficient to sustain plant productivity without agronomic P inputs. However, the low nutrient requirements of highly efficient lignocellulosic perennials limited the response of miscanthus productivity and NUE to basalt-derived P inputs, making impacts on N_2O emissions from miscanthus negligible (Figures 8 and 10; Table 1; Davis et al., 2010, 2015; Hudiburg et al., 2015). Consistently, net N_2O fluxes were responsive to P availability in maize but not in miscanthus (Figure 9).

The incorporation of basalt additions into routine agronomic practices could significantly abate the N_2O EF of cropping systems, but the effect varied with the soil properties of amended croplands and crop nutrient cycle efficiencies that dictate fertilizer requirements (Figure 10). Soil texture, organic matter content, and initial soil pH are strong determinants of the pH buffering capacity and hence dictate the susceptibility of a given soil to pH alterations. Basalt-induced decreases in soil acidity and subsequent impacts on the N_2O EF of cultivated soils will be greatest in low organic, coarsely textured acidic soils, which are common consequences of long-term intensive agricultural practices. Similarly, how responsive N_2O emissions from cultivated land are to basalt-driven increases in soil P availability depends on initial levels of bioavailable P and crop nutrient requirements.

At present, P deficits cover almost 30% of the global cropland despite agronomic inputs exceeding P removal by harvested crops (MacDonald et al., 2011). Limited P availability may result from low retention in soils in highly weathered soils and poor plant uptake efficiency, as P in soils exists predominantly in inorganic fractions that are only sparingly available to plants (Richardson & Simpson, 2011). Repeated P fertilization together with low P retention or excessive accumulation in unavailable forms has led to P losses from cultivated soils to water bodies causing the eutrophication

of agricultural watersheds (Goyette et al., 2018). Our simulations suggest that the synergistic effect between basalt-induced increases in soil pH and P additions, both on N₂O fluxes and the productivity of maize, was likely caused by the combined effect of enhanced inorganic P dissolution and organic P mineralization into bioavailable forms in less acidic soils, and subsequent increases in plant nutrient uptake (Figure 8; Table 1; Glaser & Lehr, 2019; Penn & Camberato, 2019). By providing a slow-release P source and promoting both, the adsorption and efficient mobilization of phosphates by cation release and soil alkalization (Anda et al., 2015; Gillman et al., 2002; Kelland et al., 2020), routine basalt additions may help avert P losses by runoff and leaching, and replace the use of P fertilizers while reducing the N₂O EF and increasing the ANR and NUE of heavily managed crops.

In summary, the addition of new subroutines to DayCent relating key elements of the nitrogen and phosphorus cycles to soil pH, improved the accuracy of model predictions of N₂O fluxes from agricultural soils. Our results from the improved model predict that the large-scale deployment of basalt, by reducing the N₂O EF of cropping systems could effectively contribute to the sustainable intensification of agriculture and enhance the climate mitigation potential of BECCS strategies significantly. Roughly 40% of today's US maize production is used for bioethanol, and lignocellulosic perennial crops such as miscanthus are rapidly expanding as high-yielding second-generation bioenergy sources (Davis et al., 2012; Hudiburg et al., 2016). The routine amendment of bioenergy crops with basalt provides an opportunity to reduce the non-CO₂ climate forcing of biofuels, while reducing nutrient overuse and increasing yields of underperforming cropland. However, the strong dependence of N₂O response dynamics on changes in soil pH and available P imply an asymmetric distribution of climate savings with basalt additions. Trade-offs related with the large-scale deployment of basalt amendments need to be further assessed to characterizing the potential for climate mitigation more reliably and geographically explicitly.

ACKNOWLEDGEMENTS

This paper is a product of the Leverhulme Centre for Climate Change Mitigation, funded by the Leverhulme Trust through a Research Centre award (RC-2015-029). Additional support was provided by the DOE Center for Advanced Bioenergy and Bioproducts Innovation (US Department of Energy, Office of Science, Office of Biological and Environmental Research under award number DE-SC 18420). Collection of maize and miscanthus yield data from control plots were supported by CABBI, DOE. The datasets generated during and/or analyzed during the current study as well as related computer code are available from the corresponding author on reasonable request.

AUTHORS' CONTRIBUTIONS

E.B.-B., I.B.K., D.J.B., and E.H.D. conceived and designed the experiments; E.B.-B., N.G.-C., M.D.H., and W.J.P. designed and implemented model improvements; E.B.-B. conducted the modeling exercises; A.L.L. characterized the basalts; and E.B.-B., I.B.K., N.G.-C., D.J.B., and E.H.D. wrote the manuscript.

DATA AVAILABILITY STATEMENT

The data that support the findings of this study and modified model code are available from the corresponding author upon reasonable request.

ORCID

Elena Blanc-Betes  <https://orcid.org/0000-0002-2049-4613>

Nuria Gomez-Casanovas  <https://orcid.org/0000-0003-4784-3585>

David J. Beerling  <https://orcid.org/0000-0003-1869-4314>

Evan H. DeLucia  <https://orcid.org/0000-0003-3400-6286>

REFERENCES

- Abdalla, M., Jones, M., Yeluripati, J., Smith, P., Burke, J., & Williams, M. (2010). Testing DAYCENT and DNDC model simulations of N₂O fluxes and assessing the impacts of climate change on the gas flux and biomass production from a humid pasture. *Atmospheric Environment*, 44, 2961–2970. <https://doi.org/10.1016/j.atmosenv.2010.05.018>
- Ågren, G. I., Wetterstedt, J. Å. M., & Billberger, M. F. K. (2012). Nutrient limitation on terrestrial plant growth – Modeling the interaction between nitrogen and phosphorus. *New Phytologist*, 194(4), 953–960. <https://doi.org/10.1111/j.1469-8137.2012.04116.x>
- Anda, M., Shamshuddin, J., & Fauziah, C. I. (2015). Improving chemical properties of a highly weathered soil using finely ground basalt rocks. *Catena*, 124, 147–161. <https://doi.org/10.1016/j.catena.2014.09.012>
- Anderson-Teixeira, K. J., Davis, S. C., Masters, M. D., & DeLucia, E. H. (2009). Changes in soil organic carbon under biofuel crops. *GCB Bioenergy*, 1, 75–96. <https://doi.org/10.1111/j.1757-1707.2008.01001.x>
- Arundale, R. A., Dohleman, F. G., Heaton, E. A., & Mcgrath, J. M. (2014). Yields of *Miscanthus × giganteus* and *Panicum virgatum* decline with stand age in the Midwestern USA. *GCB Bioenergy*, 6, 1–13. <https://doi.org/10.1111/gcbb.12077>
- Arundale, R. A., Dohleman, F. G., Voigt, T. B., & Long, S. P. (2014). Nitrogen fertilization does significantly increase yields of stands of *Miscanthus × giganteus* and *Panicum virgatum* in multiyear trials in Illinois. *BioEnergy Research*, 7, 408–416. <https://doi.org/10.1007/s12155-013-9385-5>
- Baral, B. R., Kuyper, T. W., & Van Groenigen, J. W. (2014). Liebig's law of the minimum applied to a greenhouse gas: Alleviation of P-limitation reduces soil N₂O emission. *Plant and Soil*, 374, 539–548. <https://doi.org/10.1007/s11104-013-1913-8>
- Beerling, D. J., Leake, J. R., Long, S. P., Scholes, J. D., Ton, J., Nelson, P. N., Bird, M., Kantzas, E., Taylor, L. L., Sarkar, B., Kelland, M., DeLucia, E., Kantola, I., Müller, C., Rau, G., & Hansen, J. (2018). Farming with crops and rocks to address global climate, food and soil security. *Nature Plants*, 4(3), 138–147. <https://doi.org/10.1038/s41477-018-0108-y>

- Cabeza, R. A., Myint, K., Steingrobe, B., Stritsis, C., Schulze, J., & Claassen, N. (2017). Phosphorus fractions depletion in the rhizosphere of young and adult maize and oilseed rape plants. *Journal of Soil Science and Plant Nutrition*, 17, 824–838. <https://doi.org/10.4067/S0718-95162017000300020>
- Campbell, E. E., Johnson, J. M. F., Jin, V. L., Lehman, R. M., Osborne, S. L., Varvel, G. E., & Paustian, K. (2014). Assessing the soil carbon, biomass production, and nitrous oxide emission impact of corn stover management for bioenergy feedstock production using DAYCENT. *BioEnergy Research*, 7, 491–502. <https://doi.org/10.1007/s12155-014-9414-z>
- Cao, P., Lu, C., & Yu, Z. (2018). Historical nitrogen fertilizer use in agricultural ecosystems of the contiguous United States during 1850–2015: Application rate, timing, and fertilizer types. *Earth System Science Data*, 10, 969–984. <https://doi.org/10.5194/essd-10-969-2018>
- Cheng, K., Ogle, S. M., Parton, W. J., & Pan, G. (2014). Simulating greenhouse gas mitigation potentials for Chinese Croplands using the DAYCENT ecosystem model. *Global Change Biology*, 20, 948–962. <https://doi.org/10.1111/gcb.12368>
- Christian, D. G., Riche, A. B., & Yates, N. E. (2008). Growth, yield and mineral content of *Miscanthus × giganteus* grown as a biofuel for 14 successive harvests. *Industrial Crops and Products*, 28, 320–327. <https://doi.org/10.1016/j.indcrop.2008.02.009>
- Crutzen, P. J., Mosier, A. R., Smith, K. A., & Winiwarter, W. (2016). N₂O release from agro-biofuel production negates global warming reduction by replacing fossil fuels. In: P. J. Crutzen & H. G. Brauch (Eds.), *Paul J. Crutzen: A pioneer on atmospheric chemistry and climate change in the Anthropocene* (pp. 227–238). Springer International Publishing.
- Davidson, E. A. (2009). The contribution of manure and fertilizer nitrogen to atmospheric nitrous oxide since 1860. *Nature Geoscience*, 2, 659–662. <https://doi.org/10.1038/ngeo608>
- Davidson, E. A., & Kanter, D. (2014). Inventories and scenarios of nitrous oxide emissions. *Environmental Research Letters*, 9, 105012. <https://doi.org/10.1088/1748-9326/9/10/105012>
- Davis, M. P., David, M. B., Voigt, T. B., & Mitchell, C. A. (2015). Effect of nitrogen addition on *Miscanthus × giganteus* yield, nitrogen losses, and soil organic matter across five sites. *GCB Bioenergy*, 7, 1222–1231. <https://doi.org/10.1111/gcbb.12217>
- Davis, S. C., Parton, W. J., Dohleman, F. G., Smith, C. M., Del Grosso, S., Kent, A. D., & DeLucia, E. H. (2010). Comparative biogeochemical cycles of bioenergy crops reveal nitrogen-fixation and low greenhouse gas emissions in a *Miscanthus × giganteus* agro-ecosystem. *Ecosystems*, 13, 144–156. <https://doi.org/10.1007/s10021-009-9306-9>
- Davis, S. C., Parton, W. J., Grosso, S. J. D., Keough, C., Marx, E., Adler, P. R., & DeLucia, E. H. (2012). Impact of second-generation biofuel agriculture on greenhouse-gas emissions in the corn-growing regions of the US. *Frontiers in Ecology and the Environment*, 10, 69–74. <https://doi.org/10.1890/110003>
- De Klein, C., Novoa, R. S. A., Ogle, S., Smith, K. A., Rochette, P., Wirth, T. C., McConkey, B., Mosier, A. R., & Rypdal, K. (2006). *IPCC guidelines for national greenhouse gas inventories, Volume 4, Chapter 11: N₂O emissions from managed soils, and CO₂ emissions from lime and urea application*. Technical report 4-88788-032-4. Intergovernmental Panel on Climate Change.
- Del Grosso, S. J., Halvorson, A. D., & Parton, W. J. (2008). Testing DAYCENT model simulations of corn yields and nitrous oxide emissions in irrigated tillage systems in Colorado. *Journal of Environmental Quality*, 37, 1383–1389. <https://doi.org/10.2134/jeq2007.0292>
- Del Grosso, S. J., Mosier, A. R., Parton, W. J., & Ojima, D. S. (2005). DAYCENT model analysis of past and contemporary soil N₂O and net greenhouse gas flux for major crops in the USA. *Soil & Tillage Research*, 83, 9–24. <https://doi.org/10.1016/j.still.2005.02.007>
- Del Grosso, S. J., Ogle, S. M., Parton, W. J., & Breidt, F. J. (2010). Estimating uncertainty in N₂O emissions from U.S. cropland soils. *Global Biogeochemical Cycles*, 24. <https://doi.org/10.1029/2009GB003544>
- Del Grosso, S. J., Ojima, D. S., Parton, W. J., Stehfest, E., Heistemann, M., DeAngelo, B., & Rose, S. (2009). Global scale DAYCENT model analysis of greenhouse gas emissions and mitigation strategies for cropped soils. *Global and Planetary Change*, 67, 44–50. <https://doi.org/10.1016/j.gloplacha.2008.12.006>
- Del Grosso, S. J., Parton, W. J., Mosier, A. R., Hartman, M. D., Brenner, J., Ojima, D. S., & Schimel, D. S. (2001). Simulated interaction of carbon dynamics and nitrogen trace gas fluxes using the DAYCENT model. *Model Carbon and Nitrogen Dynamics for Soil Management*, 303–332. <https://doi.org/10.1201/9781420032635.ch8>
- Del Grosso, S. J., Parton, W. J., Mosier, A. R., Ojima, D. S., Kulmala, A. E., & Phongpan, S. (2000). General model for N₂O and N₂ gas emissions from soils due to denitrification. *Global Biogeochemical Cycles*, 14, 1045–1060. <https://doi.org/10.1029/1999GB001225>
- Del Grosso, S. J., Parton, W. J., Mosier, A. R., Walsh, M. K., Ojima, D. S., & Thornton, P. E. (2006). DAYCENT national-scale simulations of nitrous oxide emissions from cropped soils in the United States. *Journal of Environmental Quality*, 35, 1451–1460. <https://doi.org/10.2134/jeq2005.0160>
- Del Grosso, S. J., Parton, W. J., Stohlgren, T., Zheng, D., Bachelet, D., Prince, S., Hibbard, K., & Olson, R. (2008). Global potential net primary production predicted from vegetation class, precipitation, and temperature. *Ecology*, 89, 2117–2126. <https://doi.org/10.1890/07-0850.1>
- Del Grosso, S. J., Wirth, T., Ogle, S. M., & Parton, W. J. (2008). Estimating agricultural nitrous oxide emissions. *Eos, Transactions American Geophysical Union*, 89, 529. <https://doi.org/10.1029/2008EO510001>
- Del Grosso, S. J., Parton, W. J., Keough, C. A., & Reyes-Fox, M. (2011). Special features of the DAYCENT modeling package and additional procedures for parameterization, calibration, validation, and applications. In *Methods of introducing system models into agricultural research* (pp. 155–176). <https://doi.org/10.2134/advagricsysmod.el2.c5>
- Del Grosso, S. J., Parton, W. J., Mosier, A. R., Hartman, M. D., Keough, C. A., Peterson, G. A., Ojima, D. S., & Schimel, D. S. (2001). Simulated effects of land use, soil texture, and precipitation on N gas emissions using DAYCENT. In *Nitrogen in the environment: Sources, problems and management* (pp. 413–431). Elsevier Science Publ.
- Dohleman, F. G., Heaton, E. A., Arundale, R. A., & Long, S. P. (2012). Seasonal dynamics of above- and below-ground biomass and nitrogen partitioning in *Miscanthus × giganteus* and *Panicum virgatum* across three growing seasons. *GCB Bioenergy*, 4, 534–544. <https://doi.org/10.1111/j.1757-1707.2011.01153.x>
- Fageria, N. K., & Baligar, V. C. (2005). Enhancing nitrogen use efficiency in crop plants. *Advances in agronomy*, 88, 97–185. [https://doi.org/10.1016/S0065-2113\(05\)88004-6](https://doi.org/10.1016/S0065-2113(05)88004-6)
- Faucon, M.-P., Houben, D., Reynoird, J.-P., Mercadal-Dulaurent, A. M., Armand, R., & Lambers, H. (2015). Advances and perspectives

- to improve the phosphorus availability in cropping systems for agroecological phosphorus management. In D. L. Sparks (Ed.), *Advances in agronomy* (Vol. 134, pp. 51–79). Elsevier Science Publ.
- Foster, B. L., Murphy, C. A., Keller, K. R., Aschenbach, T. A., Questad, E. J., & Kindscher, K. (2007). Restoration of prairie community structure and ecosystem function in an abandoned hayfield: A sowing experiment. *Restoration Ecology*, 15, 652–661. <https://doi.org/10.1111/j.1526-100X.2007.00277.x>
- Fuss, S., Canadell, J. G., Peters, G. P., Tavoni, M., Andrew, R. M., Ciais, P., Jackson, R. B., Jones, C. D., Kraxner, F., Nakicenovic, N., Le Quéré, C., Raupach, M. R., Sharifi, A., Smith, P., & Yamagata, Y. (2014). Betting on negative emissions. *Nature Climate Change*, 4, 850–853. <https://doi.org/10.1038/nclimate2392>
- Gillman, G. P., Burkett, D. C., & Coventry, R. J. (2001). A laboratory study of application of basalt dust to highly weathered soils: Effect on soil cation chemistry. *Soil Research*, 39, 799–811. <https://doi.org/10.1071/sr00073>
- Gillman, G. P., Burkett, D. C., & Coventry, R. J. (2002). Amending highly weathered soils with finely ground basalt rock. *Applied Geochemistry*, 17, 987–1001. [https://doi.org/10.1016/S0883-2927\(02\)00078-1](https://doi.org/10.1016/S0883-2927(02)00078-1)
- Glaser, B., & Lehr, V.-I. (2019). Biochar effects on phosphorus availability in agricultural soils: A meta-analysis. *Scientific Reports*, 9. <https://doi.org/10.1038/s41598-019-45693-z>
- Goyette, J.-O., Bennett, E. M., & Maranger, R. (2018). Low buffering capacity and slow recovery of anthropogenic phosphorus pollution in watersheds. *Nature Geoscience*, 11, 921–925. <https://doi.org/10.1038/s41561-018-0238-x>
- Heaton, E. A., Dohleman, F. G., & Long, S. P. (2009). Seasonal nitrogen dynamics of *Miscanthus × giganteus* and *Panicum virgatum*. *GCB Bioenergy*, 1, 297–307. <https://doi.org/10.1111/j.1757-1707.2009.01022.x>
- Hénault, C., Bourennane, H., Ayzac, A., Ratié, C., Saby, N. P. A., Cohan, J.-P., Eglin, T., & Gall, C. L. (2019). Management of soil pH promotes nitrous oxide reduction and thus mitigates soil emissions of this greenhouse gas. *Scientific Reports*, 9, 1–11. <https://doi.org/10.1038/s41598-019-56694-3>
- Hudiburg, T. W., Davis, S. C., Parton, W., & DeLucia, E. H. (2015). Bioenergy crop greenhouse gas mitigation potential under a range of management practices. *GCB Bioenergy*, 7, 366–374. <https://doi.org/10.1111/gcbb.12152>
- Hudiburg, T. W., Wang, W., Khanna, M., Long, S. P., Dwivedi, P., Parton, W. J., Hartman, M., & DeLucia, E. H. (2016). Impacts of a 32-billion-gallon bioenergy landscape on land and fossil fuel use in the US. *Nature Energy*, 1(1). <https://doi.org/10.1038/nenergy.2015.5>
- Inatomi, M., Hajima, T., & Ito, A. (2019). Fraction of nitrous oxide production in nitrification and its effect on total soil emission: A meta-analysis and global-scale sensitivity analysis using a process-based model. *PLOS ONE*, 14(7), e0219159. <https://doi.org/10.1371/journal.pone.0219159>
- Kantola, I. B., Blanc-Betes, E., Masters, M. D., Val Martin, M., Bernacchi, C. J., & Beerling, D. J., & DeLucia, E. H. (in review). Basalt application for carbon sequestration reduces nitrous oxide fluxes from croplands. *Ecosystems*.
- Kantola, I. B., Masters, M. D., & DeLucia, E. H. (2017). Soil particulate organic matter increases under perennial bioenergy crop agriculture. *Soil Biology and Biochemistry*, 113, 184–191. <https://doi.org/10.1016/j.soilbio.2017.05.023>
- Kato, E., & Yamagata, Y. (2014). BECCS capability of dedicated bioenergy crops under a future land-use scenario targeting net negative carbon emissions. *Earths Future*, 2, 421–439. <https://doi.org/10.1002/2014EF000249>
- Kelland, M. E., Wade, P. W., Lewis, A. L., Taylor, L. L., Sarkar, B., Andrews, M. G., Lomas, M. R., Cotton, T. A., Kemp, S. J., James, R. H., & Pearce, C. R. (2020). Increased yield and CO₂ sequestration potential with the C₄ cereal *Sorghum bicolor* cultivated in basaltic rock dust-amended agricultural soil. *Global Change Biology*, 26, 3658–3676. <https://doi.org/10.1111/gcb.15089>
- Kelly, R. H., Parton, W. J., Crocker, G. J., Graced, P. R., Klír, J., Körschens, M., Poulton, P. R., & Richter, D. D. (1997). Simulating trends in soil organic carbon in long-term experiments using the century model. *Geoderma*, 81(1), 75–90. [https://doi.org/10.1016/S0016-7061\(97\)00082-7](https://doi.org/10.1016/S0016-7061(97)00082-7)
- Kelly, R. H., Parton, W. J., Hartman, M. D., Stretch, L. K., Ojima, D. S., & Schimel, D. S. (2000). Intra-annual and interannual variability of ecosystem processes in shortgrass steppe. *Journal of Geophysical Research: Atmospheres*, 105(D15), 20093–20100. <https://doi.org/10.1029/2000JD900259>
- Krichels, A., DeLucia, E. H., Sanford, R., Chee-Sanford, J., & Yang, W. H. (2019). Historical soil drainage mediates the response of soil greenhouse gas emissions to intense precipitation events. *Biogeochemistry*, 142, 425–442. <https://doi.org/10.1007/s10533-019-00544-x>
- Lee, M.-S., Wycislo, A., Guo, J., Lee, D. K., & Voigt, T. (2017). Nitrogen fertilization effects on biomass production and yield components of *Miscanthus × giganteus*. *Frontiers in Plant Science*, 8. <https://doi.org/10.3389/fpls.2017.00544>
- Liu, B., Mørkved, P. T., Frostegård, Å., & Bakken, L. R. (2010). Denitrification gene pools, transcription and kinetics of NO, N₂O and N₂ production as affected by soil pH. *FEMS Microbiology Ecology*, 72, 407–417. <https://doi.org/10.1111/j.1574-6941.2010.00856.x>
- MacDonald, G. K., Bennett, E. M., Potter, P. A., & Ramankutty, N. (2011). Agronomic phosphorus imbalances across the world's croplands. *Proceedings of the National Academy of Sciences of the United States of America*, 108, 3086–3091. <https://doi.org/10.1073/pnas.1010808108>
- McMillan, A. M. S., Pal, P., Phillips, R. L., Palmada, T., Berben, P. H., Jha, N., Saggar, S., & Luo, J. (2016). Can pH amendments in grazed pastures help reduce N₂O emissions from denitrification? The effects of liming and urine addition on the completion of denitrification in fluvial and volcanic soils. *Soil Biology and Biochemistry*, 93, 90–104. <https://doi.org/10.1016/j.soilbio.2015.10.013>
- Mehnaz, K. R., Keitel, C., & Dijkstra, F. A. (2018). Effects of carbon and phosphorus addition on microbial respiration, N₂O emission, and gross nitrogen mineralization in a phosphorus-limited grassland soil. *Biology and Fertility of Soils*, 54, 481–493. <https://doi.org/10.1007/s00374-018-1274-9>
- Mukumbuta, I., Uchida, Y., & Hatano, R. (2018). Evaluating the effect of liming on N₂O fluxes from denitrification in an Andosol using the acetylene inhibition and ¹⁵N isotope tracer methods. *Biology and Fertility of Soils*, 54, 71–81. <https://doi.org/10.1007/s00374-017-1239-4>
- NASS (National Agricultural Statistics Service). (2019). *Census of Agriculture Quick Stats 2.0 Beta*. United States Department of Agriculture. Retrieved from <https://quickstats.nass.usda.gov/>
- Obersteiner, M., Bednar, J., Wagner, F., Gasser, T., Ciais, P., Forsell, N., Frank, S., Havlik, P., Valin, H., Janssens, I. A., Peñuelas, J., & Schmidt-Traub, G. (2018). How to spend a dwindling greenhouse gas budget. *Nature Climate Change*, 8, 7. <https://doi.org/10.1038/s41558-017-0045-1>

- Parton, W. J., Hartman, M., Ojima, D., & Schimel, D. (1998). DAYCENT and its land surface submodel: Description and testing. *Global and Planetary Change*, 19, 35–48. [https://doi.org/10.1016/S0921-8181\(98\)00040-X](https://doi.org/10.1016/S0921-8181(98)00040-X)
- Parton, W. J., Holland, E. A., Del Grosso, S. J., Hartman, M. D., Martin, R. E., Mosier, A. R., Ojima, D. S., & Schimel, D. S. (2001). Generalized model for NO_x and N₂O emissions from soils. *Journal of Geophysical Research: Atmospheres*, 106, 17403–17419. <https://doi.org/10.1029/2001JD900101>
- Parton, W. J., Mosier, A. R., Ojima, D. S., Valentine, D. W., Schimel, D. S., Weier, K., & Kulmala, A. E. (1996). Generalized model for N₂ and N₂O production from nitrification and denitrification. *Global Biogeochemical Cycles*, 10, 401–412. <https://doi.org/10.1029/96GB01455>
- Parton, W. J., Ojima, D. S., Cole, C. V., & Schimel, D. S. (1994). A general model for soil organic matter dynamics: Sensitivity to litter chemistry, texture and management. In *Quantitative modeling of soil forming processes* (Vol. 39, pp. 147–167). John Wiley & Sons, Ltd. <https://doi.org/10.2136/sssaspecpub39.c9>
- Parton, W. J., Scurlock, J. M. O., Ojima, D. S., Gilmanov, T. G., Scholes, R. J., Schimel, D. S., Kirchner, T., Menaut, J.-C., Seastedt, T., Moya, E. G., Kamnalrut, A., & Kinyamario, J. I. (1993). Observations and modeling of biomass and soil organic matter dynamics for the grassland biome worldwide. *Global Biogeochemical Cycles*, 7(4), 785–809. <https://doi.org/10.1029/93GB02042>
- Penn, C. J., & Camberato, J. J. (2019). A critical review on soil chemical processes that control how soil pH affects phosphorus availability to plants. *Agriculture*, 9, 120. <https://doi.org/10.3390/agriculture9060120>
- Potter, C. S., Matson, P. A., Vitousek, P. M., & Davidson, E. A. (1996). Process modeling of controls on nitrogen trace gas emissions from soils worldwide. *Journal of Geophysical Research: Atmospheres*, 101, 1361–1377. <https://doi.org/10.1029/95JD02028>
- Reay, D. S., Davidson, E. A., Smith, K. A., Melillo, J. M., Dentener, F., & Crutzen, P. J. (2012). Global agriculture and nitrous oxide emissions. *Nature Climate Change*, 2, 410–416. <https://doi.org/10.1038/nclimate1458>
- Richardson, A. E., & Simpson, R. J. (2011). Soil microorganisms mediating phosphorus availability update on microbial phosphorus. *Plant Physiology*, 156, 989–996. <https://doi.org/10.1104/pp.111.175448>
- Rochester, I. J. (2003). Estimating nitrous oxide emissions from flood-irrigated alkaline grey clays. *Soil Research*, 41, 197–206. <https://doi.org/10.1071/sr02068>
- Samad, M. S., Bakken, L. R., Nadeem, S., Clough, T. J., de Klein, C. A. M., Richards, K. G., Lanigan, G. J., & Morales, S. E. (2016). High-resolution denitrification kinetics in pasture soils link N₂O emissions to pH, and denitrification to C mineralization. *PLoS One*, 11, e0151713. <https://doi.org/10.1371/journal.pone.0151713>
- Schlegel, A. J., Dhuyvetter, K. C., & Havlin, J. L. (1996). Economic and environmental impacts of long-term nitrogen and phosphorus fertilization. *Journal of Production Agriculture*, 9, 114–118. <https://doi.org/10.2134/jpa1996.0114>
- Shcherbak, I., Millar, N., & Robertson, G. P. (2014). Global metaanalysis of the nonlinear response of soil nitrous oxide (N₂O) emissions to fertilizer nitrogen. *Proceedings of the National Academy of Sciences of the United States of America*, 111, 9199–9204. <https://doi.org/10.1073/pnas.1322434111>
- Šimek, M., & Cooper, J. E. (2002). The influence of soil pH on denitrification: progress towards the understanding of this interaction over the last 50 years. *European Journal of Soil Science*, 53, 345–354. <https://doi.org/10.1046/j.1365-2389.2002.00461.x>
- Šimek, M., Jiřová, L., & Hopkins, D. W. (2002). What is the so-called optimum pH for denitrification in soil? *Soil Biology and Biochemistry*, 34, 1227–1234. [https://doi.org/10.1016/S0038-0717\(02\)00059-7](https://doi.org/10.1016/S0038-0717(02)00059-7)
- Smith, P., Adams, J., Beerling, D. J., Beringer, T., Calvin, K. V., Fuss, S., Griscom, B., Hagemann, N., Kammann, C., Kraxner, F., Minx, J. C., Popp, A., Renforth, P., Vicente Vicente, J. L., & Keesstra, S. (2019). Land-management options for greenhouse gas removal and their impacts on ecosystem services and the Sustainable Development Goals. *Annual Review of Environment and Resources*, 44, 255–286. <https://doi.org/10.1146/annurev-environ-101718-033129>
- Smith, C. M., David, M. D., Mitchell, C., Masters, M. D., Anderson-Teixeira, K., Bernacchi, C. J., & DeLucia, E. H. (2013). Reduced nitrogen losses after conversion of row crop agriculture to perennial biofuel crops. *Journal of Environmental Quality*, 42(1), 219–228. <https://doi.org/10.2134/jeq2012.0210>
- Smith, P., Davis, S. J., Creutzig, F., Fuss, S., Minx, J., Gabrielle, B., Kato, E., Jackson, R. B., Cowie, A., Kriegler, E., van Vuuren, D. P., Rogelj, J., Ciais, P., Milne, J., Canadell, J. G., McCollum, D., Peters, G., Andrew, R., Krey, V., ... Yongsung, C. (2016). Biophysical and economic limits to negative CO₂ emissions. *Nature Climate Change*, 6, 42–50. <https://doi.org/10.1038/nclimate2870>
- Taylor, L. L., Quirk, J., Thorley, R. M. S., Kharecha, P. A., Hansen, J., Ridgwell, A., Lomas, M. R., Banwart, S. A., & Beerling, D. J. (2016). Enhanced weathering strategies for stabilizing climate and averting ocean acidification. *Nature Climate Change*, 6, 402–406. <https://doi.org/10.1038/nclimate2882>
- Thornton, P. E., Thornton, M. M., Mayer, B. W., Wilhelmi, N., Wei, Y., Devarakonda, R., & Cook, R. B. (2016). *Daymet: Daily surface weather data on a 1-km grid for North America, Version 3*. ORNL DAAC. <https://doi.org/10.3334/ORNLDAAAC/1328>
- Tilman, D., Balzer, C., Hill, J., & Belfort, B. L. (2011). Global food demand and the sustainable intensification of agriculture. *Proceedings of the National Academy of Sciences of the United States of America*, 108, 20260–20264. <https://doi.org/10.1073/pnas.1116437108>
- USDA, Economic Research Service. (2019). *Fertilizer use and price*. Retrieved from <https://www.ers.usda.gov/data-products/fertilizer-use-and-price.aspx>
- USGS. (2003). Geologic Map of Virginia. Virginia Division of Mineral Resources. Retrieved from <https://mrdata.usgs.gov/geology/>
- Viovy, N. (2018). CRUNCEP version 7 – atmospheric forcing data for the community land model. Research data archive at the National Center for Atmospheric Research, Computational and Information Systems Laboratory. Retrieved from <https://rda.ucar.edu/datasets/ds314.3/>
- Wagena, M. B., Bock, E. M., Sommerlot, A. R., Fuka, D. R., & Easton, Z. M. (2017). Development of a nitrous oxide routine for the SWAT model to assess greenhouse gas emissions from agroecosystems. *Environmental Modelling and Software*, 89, 131–143. <https://doi.org/10.1016/j.envsoft.2016.11.013>
- Wang, Y., Guo, J., Vogt, R. D., Mulder, J., Wang, J., & Zhang, X. (2018). Soil pH as the chief modifier for regional nitrous oxide emissions: New evidence and implications for global estimates and mitigation. *Global Change Biology*, 24, e617–e626. <https://doi.org/10.1111/gcb.13966>
- Xu-Ri, Prentice, I. C., Spahni, R., & Niu, H. S. (2012). Modelling terrestrial nitrous oxide emissions and implications for climate feedback. *New Phytologist*, 196, 472–488. <https://doi.org/10.1111/j.1469-8137.2012.04269.x>

Yu, L., Wang, Y., Zhang, X., Dörsch, P., & Mulder, J. (2017). Phosphorus addition mitigates N₂O and CH₄ emissions in N-saturated subtropical forest, SW China. *Biogeosciences*, *14*, 3097–3109. <https://doi.org/10.5194/bg-14-3097-2017>

SUPPORTING INFORMATION

Additional supporting information may be found online in the Supporting Information section.

How to cite this article: Blanc-Betes E, Kantola IB, Gomez-Casanovas N, et al. In silico assessment of the potential of basalt amendments to reduce N₂O emissions from bioenergy crops. *GCB Bioenergy*. 2020;00:1–18. <https://doi.org/10.1111/gcbb.12757>